Transient Burned Gas Rate Control on VVA equipped Diesel Engines

T. Leroy * **J. Chauvin** * **N. Petit** **

* *IFP, Department of Engine Control, 1 et 4 Avenue de Bois Préau, 92852 Rueil Malmaison, France.*
** *Centre Automatique et Systèmes, Mines ParisTech, 60, bd St Michel, 75272 Paris, France.*

Abstract: This paper addresses the problem of cylinder burned gas rate transient control of VVA equipped Diesel engines. This problem is of importance for NO_x emissions reduction. The proposed strategy coordinates existing low-level intake manifold burned gas rate and VVA controllers. To determine relevant control actions, a model of cylinder filling phenomenon is determined. It expresses, under the form of a discrete event dynamics, the behavior of the cylinder burned gas rate at intake valve closure. Interestingly, the model is invertible, thanks to its analytical nature. This property directly suggests an inverse formula that serves as control law. The strategy is efficient as is highlighted by experimental results obtained on a 1.6 L Diesel engine test bench. As a result, NO_x emissions are largely diminished during transients.

Keywords: Diesel engine, NO_x emissions, Burned Gas Rate control, VVA, Model-based control

1. INTRODUCTION

Upcoming Diesel engines emission standards such as Euro 6 require significant reduction of smoke, HC (Hydrocarbons), CO (Carbon monoxide) and above all NO_x (Nitrogen Oxides) emissions. This has spurred an interest in new (cleaner) combustion modes. The premixed combustion modes (LTC: Low Temperature Combustion) represent a relatively simple and affordable solution to reduce the emissions while retaining the advantages of the Diesel engine. These modes consist of incorporating large amounts of Exhaust Gas Recirculation (EGR) into the combustion process.

Usually, the EGR can be realized in two possible manners: through a High Pressure (HP) or a Low Pressure (LP) EGR circuit. The LP EGR technology (which is considered in this paper, as pictured in Figure 1) possesses many advantages over the HP EGR circuit. In this technology, the exhaust gases are picked up downstream the turbine and the after-treatment system. The fresh air and burned gases mix and then flow through the compressor. The advantages of LP EGR are threefold. First, due to the EGR circuit length, the intake manifold mixture temperature is lower than in the case of the HP EGR. This has a beneficial impact on the NO_x emissions. Second, higher EGR rates can be obtained because LP EGR does not have any discharge effect on the turbocharger. Third, because the recirculated gases are cleaned by the after-treatment system, there is no problem of exchanger fouling. However, one main drawback of the LP technology is the large settling time because of EGR pipe length and low inlet-outlet pressure difference.

Recently, a new way to generate EGR has emerged. On top of these technological solutions, additional improvements can be achieved using a VVA device (see Bression et al. (2008)). The VVA actuator is located on the camshaft (see Figure 1). It permits a variable exhaust valve reopening (pictured in Figure 3(b)) that drastically modifies the cylinder filling process.

As has been discussed previously, the LP EGR provides good results in terms of NO_x emissions. Nevertheless, a reduced exhaust temperature resulting from the highly diluted combustion tends to produce a sharp increase in HC and CO emissions at part load because of after treatment catalyst deactivation (see Bression et al. (2008)). The VVA actuator permits to address this problem. Indeed, the variable valve actuation system traps the gases directly inside the combustion chamber (Internal Exhaust Gas Recirculation, IEGR), therefore limiting the heat exchanges. Hence, significantly higher gas temperature levels at valve closure can be reached. This permits to activate the catalyst, and, in turn, to reduce the HC and CO emissions.

In Diesel engines, the torque production control is achieved by varying the amount of fuel injected during each cycle. The NO_x emissions is controlled by modulating the Burned Gas Rate (BGR) of the cylinder mixture before combustion (links between BGR and NO_x emissions have been largely studied in the literature, see, e.g., Heywood (1988) or Toda et al. (1976) for example). In the engine under consideration, there are two ways of admitting burned gases inside the cylinder. On the one hand, the LP EGR circuit permits to manage the BGR in the intake manifold by actuating both the EGR and the exhaust valves (see Jankovic and Kolmanovsky (1998), Chauvin et al. (2008)). Because of the length of the EGR circuit, the intake manifold BGR has a *large response time* (see Throop and Cook (1985)). On the other hand, the VVA actuator has a *fast impact* on the cylinder BGR thanks to its location in the vicinity of the cylinder.

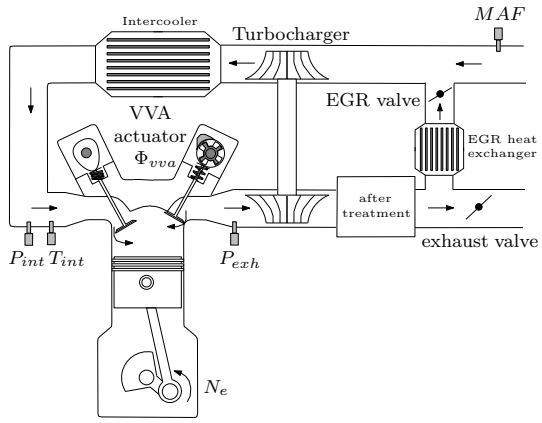

Fig. 1. Schematic illustration of a turbocharged, VVA-equipped Diesel engine. The intake manifold pressure and temperature P_{int} and T_{int}, the exhaust manifold pressure P_{exh} and the mass air flow at the intake MAF are measured by sensors. Φ_{vva} is the position of the VVA actuator.

We propose a strategy to coordinate these two sources of recirculated burned gases, such that the cylinder filling is optimized, even during transients. This is the main contribution of the paper.

The paper is organized as follows. In Section 2, we expose existing control strategies and stress their limitations. Our proposed coordination controller is outlined. It relies on a cylinder filling model which is presented in Section 3. This model has invertibility properties which are exploited in the control design of Section 4. Finally, experimental results are reported in Section 5.

2. CLASSICAL STRATEGY AND PROPOSED ADVANCED STRATEGY

2.1 Existing controllers

In classical VVA-equipped Diesel engine control strategies, a trade-off between external EGR and IEGR is formulated to minimize pollutant emissions at each engine operating point. In practice, this defines a VVA actuator position and an intake manifold BGR value. In other terms, from a torque request specified by the driver through the accelerator pedal, and from the engine speed, two-dimensional look-up tables give set points for the intake manifold BGR and the VVA actuator position controllers (see Figure 2). Implicitly, at each operating point, this defines a reference cylinder BGR and temperature.

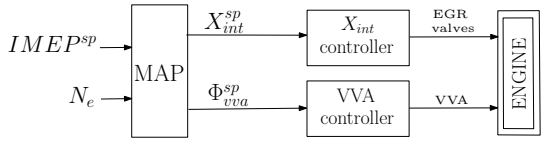

Fig. 2. Classical control strategy. $IMEP^{sp}$ and N_e refer to the driver torque demand and the engine speed, respectively. Look-up tables determine set points for the intake manifold BGR and VVA actuator position, X_{int}^{sp} and Φ_{vva}^{sp}.

The discussed intake manifold BGR and VVA actuator controllers can be considered as low-level controllers. We do not give any detail about the derivation of such controllers. Some intake manifold BGR controllers are given in Jankovic and Kolmanovsky (1998), Van Nieuwstadt et al. (2000) or Chauvin et al. (2008). Some VVA actuators controllers can be found in Chauvin and Petit (2007) or Genç et al. (2001).

Figure 3(a) represents the look-up table that gives VVA actuator position on the whole engine operating range. Figure 3(b) shows the impact of the VVA actuator on the second exhaust valve lift. It clearly appears that the second valve lift is particularly used ($\Phi_{vva} > 0$) at low and partial load to compensate for too low exhaust temperatures obtained with only external EGR.

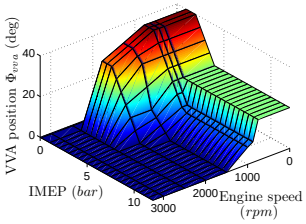

(a) Look-up table giving VVA actuator position in regards to the engine operating point.

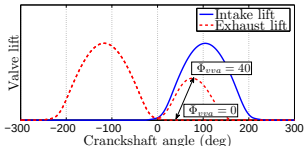

(b) VVA actuator controls the exhaust valve lift re-opening.

Fig. 3. Static positioning of the VVA actuator (Φ_{vva} stands for the VVA position) in regards to the engine operating points.

2.2 Issues during transients

Under steady operation, the above-described strategy is optimal. However, the engine is not very often under steady operation. Importantly, the dynamic responses of the intake manifold BGR and the VVA actuator are rather different. On the one hand, the response of the intake manifold BGR is quite slow (because of the EGR pipe length and the low inlet-outlet pressure difference). On the other hand, the VVA actuator dynamics is fast.

These discrepancies between the two subsystems (the intake manifold BGR and the VVA actuator) during transients lead to undesired engine behavior. Figure 4 gives results on NO_x emissions during a 3-5 bar IMEP transient. Detrimental emission peak can be observed. The two figures at the top give the intake manifold BGR and the VVA actuator position. The figure on at the bottom reports the resulting NO_x emissions. Here, the change of engine operating point modifies the intake BGR and VVA actuator position set points (more external EGR, and, consequently, less IEGR is required). Because of the intake manifold BGR sluggishness corresponding to a slow external EGR response (compared to a fast IEGR response because of the fast VVA actuator position actuation), the cylinder BGR objective is not satisfied. NO_x emission peak follows from this poor cylinder BGR control. Here, VVA actuator is not optimally used because it remains on its reference position during the transient (used as passive actuator).

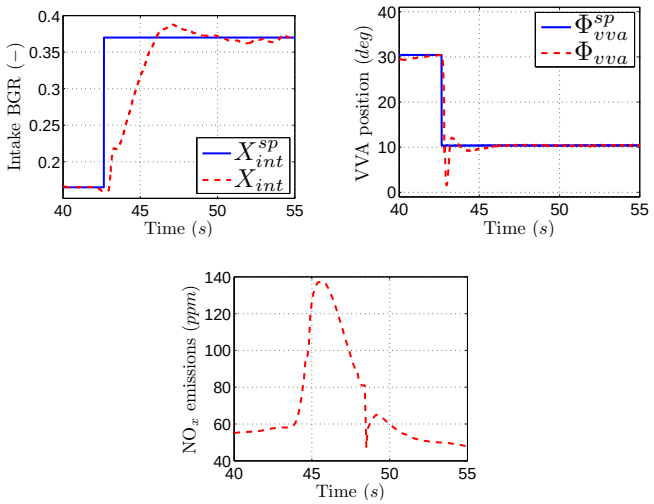

Fig. 4. Experimental IMEP transient (3-5 bar) at test bench on a 4-cylinders Diesel engine equipped with VVA actuator and LP EGR capability. The difference in response times between the intake manifold BGR and the VVA actuator leads to NO_x emission peak during transient.

2.3 Proposed advanced strategy

We propose a controller specifically designed to handle transients of VVA equipped Diesel engines. This controller focuses on compensating the difference of response times of the various dynamics of the system. We use the VVA in a very active way.

Our control objective is the cylinder BGR (which is an image of the NO_x emissions). The strategy we propose coordinates the two low-level control subsystems (intake manifold BGR and VVA actuator) to improve the cylinder BGR response. When the intake manifold BGR is too slow, the controller adjusts the VVA actuator position set point to speed up the air-feeding process, so that the cylinder BGR is satisfied. Explicitly, set point for the low-level VVA controller is determined in real time, based on estimation of the intake manifold BGR (several observers can be used to estimate this variable, as are proposed in Chauvin et al. (2008) or Wang (2008)).

3. SYSTEM MODELING

The control synthesis we propose is model-based. First, a cylinder filling model gives an estimation of the aspirated masses into the cylinder (from both the intake and the exhaust valves). Based on this analytic model, a dilution model permits to compute the cylinder BGR and temperature variables. As these dilution models require unmeasured exhaust manifold quantities (BGR and temperature), only a simple combustion model is derived.

3.1 Aspirated masses model

The quantities of aspirated masses from the intake m_{asp}^{int} (which is composed of fresh air and burned gases coming from external EGR), and from the exhaust m_{asp}^{exh} (which is composed of fresh air and burned gases coming from IEGR) are determined by the thermal conditions of the intake and exhaust manifolds (pressure, P_{int} and P_{exh}, and temperature, T_{int} and T_{exh}), the engine speed, N_e, and the positions of the VVA actuator, Φ_{vva}. Detailed model has been presented in Leroy et al. (2009). It writes

$$\begin{cases} m_{asp}^{int} = \alpha_1 \dfrac{P_{int} V_{ivc}}{R T_{int}} - \alpha_2 \dfrac{P_{exh}}{R T_{int}} V_{evc}(\Phi_{vva}) \\ m_{asp}^{exh} = \alpha_2 \dfrac{P_{exh}}{R T_{exh}} V_{evc}(\Phi_{vva}) \end{cases} \tag{1}$$

where α_1 and α_2 are known functions of N_e (this dependency is omitted hereafter for sake of conciseness). R is the ideal gas constant. V_{ivc} is the cylinder volume at intake valve closing (ivc). Similarly, V_{evc} is the cylinder volume at exhaust valve closing (evc). It is a function of the VVA actuator position, Φ_{vva} (see Figure 3(b)).

3.2 Cylinder BGR and temperature model

Conditions at intake valve closing (ivc) The cylinder BGR at ivc is equal to the mass-weighted average of the BGR of the flows contributing to the total trapped mass

$$X_{ivc}(k) = \frac{X_{int}(k) m_{asp}^{int}(k) + X_{exh}(k) m_{asp}^{exh}(k)}{m_{asp}^{int}(k) + m_{asp}^{exh}(k)} \tag{2}$$

Similarly, we assume that the cylinder temperature at ivc is equal to the mass-weighted average

$$T_{ivc}(k) = \frac{T_{int}(k) m_{asp}^{int}(k) + T_{exh}(k) m_{asp}^{exh}(k)}{m_{asp}^{int}(k) + m_{asp}^{exh}(k)} \tag{3}$$

Exhaust BGR and temperature models The models are detailed in Appendix A. For sake of conciseness, we introduce the mappings ξ and θ such that the exhaust BGR and temperature given by models (A.2) and (A.3) write

$$\begin{cases} X_{exh}(k) \triangleq \xi(X_{ivc}(k-1), T_{ivc}(k-1)) \\ T_{exh}(k) \triangleq \theta(T_{ivc}(k-1)) \end{cases} \tag{4}$$

The discrete-time nature of system (4) stems from the valves closings which isolate the cylinder from the rest of the engine. Exhaust variables are dependent to the cylinder variables of the previous combustion.

3.3 Control-oriented rewriting of the model

Let f be a mapping representing the cylinder fraction of gases coming from the IEGR. Using equations (1) and (4), it comes

$$f(\Phi_{vva}(k), \theta(T_{ivc}(k-1))) \triangleq \frac{m_{asp}^{exh}(k)}{m_{asp}^{int}(k) + m_{asp}^{exh}(k)} \tag{5}$$

Using mapping (5) into models (2) and (3) leads to the following cascade system

$$\begin{cases} X_{ivc}(k) = & f(\Phi_{vva}(k), \theta(T_{ivc}(k-1))) \\ & \cdot \xi(X_{ivc}(k-1), T_{ivc}(k-1)) \\ & + (1 - f(\Phi_{vva}(k), \theta(T_{ivc}(k-1)))) X_{int}(k) \\ T_{ivc}(k) = & f(\Phi_{vva}(k), \theta(T_{ivc}(k-1))) \theta(T_{ivc}(k-1)) \\ & + (1 - f(\Phi_{vva}(k), \theta(T_{ivc}(k-1)))) T_{int}(k) \end{cases} \tag{6}$$

Owing to the structure of V_{evc} as function of Φ_{vva}, the function f defined in (5) and appearing as a weight

for the balance equations (6) possesses some interesting invertibility properties.The following partial-invertibility property holds.

Proposition 1. For all (T_{ivc}, X_{iegr}), there exists a unique Φ_{vva} such that $f(\Phi_{vva}, \theta(T_{ivc})) = X_{iegr}$. We define the inverse function $\mathcal{F}$ such that for all T_{ivc},

$$f(\mathcal{F}(X_{iegr}, \theta(T_{ivc})), \theta(T_{ivc})) = X_{iegr} \tag{7}$$

In practice, a VVA actuator can only admit bounded values. The inversion formula appearing in (7) may produce infeasible values that need to be saturated before they can be used as input signals to the VVA control system.

4. CONTROL STRATEGY

4.1 Cylinder set points

Our control objective is to track a set point for the cylinder BGR. We define X^{sp}_{ivc} and T^{sp}_{ivc} as the set points for the cylinder BGR and temperature, respectively. They are computed from model (6), using experimentally derived look-up tables (giving set points for the intake manifold BGR and VVA actuator position, see Section 2.1). Then, the set points are obtained by solving the following equations

$$\begin{cases} X^{sp}_{ivc} = f(\Phi^{sp}_{vva}, \theta(T^{sp}_{ivc}))\xi(X^{sp}_{ivc}, T^{sp}_{ivc}) \\ \qquad\qquad + (1 - f(\Phi^{sp}_{vva}, \theta(T^{sp}_{ivc})))X^{sp}_{int} \\ T^{sp}_{ivc} = f(\Phi^{sp}_{vva}, \theta(T^{sp}_{ivc}))\theta(T^{sp}_{ivc}) \\ \qquad\qquad + (1 - f(\Phi^{sp}_{vva}, \theta(T^{sp}_{ivc})))T_{int} \end{cases} \tag{8}$$

The solution of these two equations can be analytically obtained because the system (8) is triangular. In practice, one can first compute the cylinder temperature set point T^{sp}_{ivc} by solving the second equation of system (8), using the function f defined in (5) and the aspirated masses model (1). Then, one can compute the cylinder BGR set point X^{sp}_{ivc} by substituting the obtained value of T^{sp}_{ivc} in the first equation of (8). In real applications, measurements are used in these computations (intake manifold pressure and temperature, exhaust manifold pressure and engine speed).

4.2 Coordination strategy

We propose to use the inverse model (7) to compute set points for the low-level controllers. From a cylinder BGR set point X^{sp}_{ivc}, we compute a VVA actuator position set point $\overline{\Phi_{vva}}$ by inverting the dynamic model (6), using the function $\mathcal{F}$ defined in (7). In this formula, we use an estimate of the intake manifold BGR, X_{int}. This gives

$$\overline{\Phi_{vva}}(k) = \mathcal{F}\left(\frac{X^{sp}_{ivc}(k) - X_{int}(k)}{\xi(X^{sp}_{ivc}(k-1), T^{sp}_{ivc}(k-1)) - X_{int}(k)}, \theta(T^{sp}_{ivc}(k-1))\right) \tag{9}$$

Notice that T^{sp}_{ivc} is used in place of its estimate T_{ivc} for sake of robustness. This permits to avoid creating a feedback loop in the control law. We use same measured variables (intake manifold pressure and temperature, exhaust manifold pressure and engine speed) in the control strategy (9) than in the set points computation (8). In this way, we guarantee that there is no mismatch between the set points computation and the control law.

4.3 Block structure

The presented control law (9) can be implemented under the form of the global control scheme pictured in Figure 5. The set points formulas (8) and the control strategy are implemented in the high-level controller block. This block feeds the low-level controller handling the VVA actuator. Estimation of the intake manifold BGR (X_{int}) is used in the high-level controller to coordinate the low-level controllers by means of the reference signal $\overline{\Phi_{vva}}$ determined according to (9).

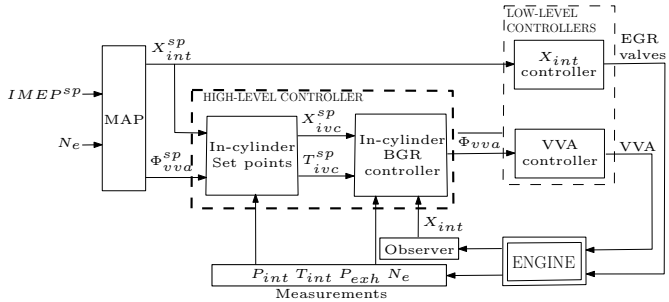

Fig. 5. Control scheme. The cylinder set points X^{sp}_{ivc} and T^{sp}_{ivc} are given in Section 4.1. The high-level controller coordinates the low-level controllers using control law presented in Section 4.2 to determine VVA actuator trajectory $\overline{\Phi_{vva}}$.

5. EXPERIMENTAL RESULTS

We now report experimental results obtained with the control law (9).

5.1 Engine setup

The engine used throughout the experiments is a 1.6 L four-cylinder direct injection HCCI-LTC Diesel engine. The second valve lift is provided by a Mechadyne^{TM} system (see Lancefield et al. (2006)) allowing a second lift between 0 and 4 *mm* (corresponding to 0 to 40 deg VVA actuator position). External EGR is carried out by a LP circuit.

5.2 Intake manifold BGR variation

The first sequence of experimental tests considers an intake manifold BGR variation, trying to keep a constant cylinder BGR. The goal of such an experiment is to validate the model validity and the control strategy under steady-state conditions. In Figure 6, the solid blue curves designate the reference control strategy (named "ref", presented in Section 2.1) and the dashed red curves refer to the proposed control strategy (named "strat", presented in Section 4.2).

Figure 6(a) reports the exhaust valve position variation trajectory that is imposed in both cases. Figure 6(c) presents the resulting intake manifold BGR response. Note

that the mismatch between the two curves arises from the differences in VVA positions between the two strategies. Figure 6(d) gives the VVA actuator trajectory. In the reference strategy, the VVA actuator is set to its mapped position according to the engine operating point. In the proposed strategy, the VVA actuator trajectory (given by the control law (9)) moves away from its reference position to satisfy the cylinder BGR demand. Figure 6(e) shows that the cylinder BGR request is kept constant during the whole test (except around 120 s because of the VVA actuator saturation). Figure 6(f) shows that the VVA actuator position variations lead to strong cylinder temperature variations. Finally, Figure 6(b) presents the NO_x emissions obtained using the two strategies. The proposed strategy succeeds in keeping the emissions constants.

This experiment highlights two facts. First, the cylinder BGR is the relevant control variable for NO_x emissions control purpose. Second, the designed cylinder composition model is consistent with reality.

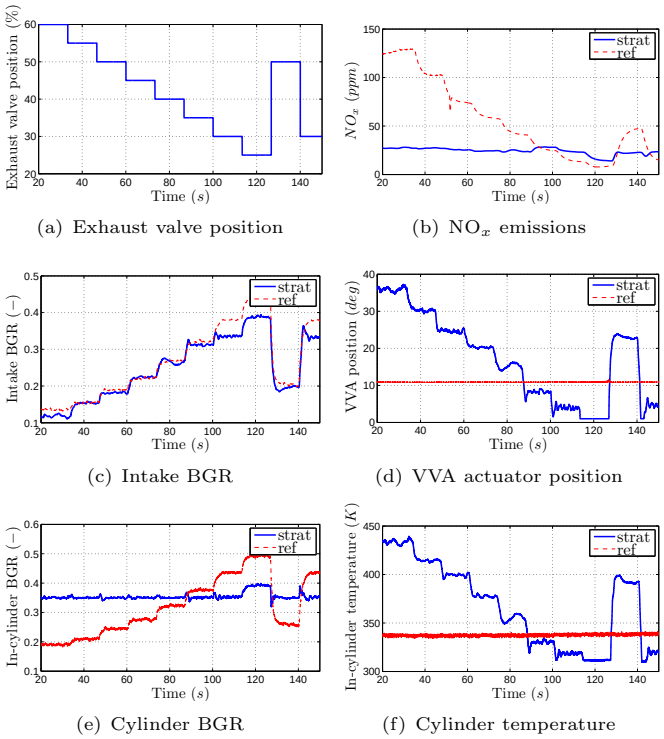

(a) Exhaust valve position (b) NO_x emissions

(c) Intake BGR (d) VVA actuator position

(e) Cylinder BGR (f) Cylinder temperature

Fig. 6. Test-bench results for a four-cylinder Diesel engine for exhaust valve position variation at constant speed of 1500 rpm with and without the proposed control strategy. The controller succeeds in keeping constant the cylinder BGR, and consequently the NO_x emissions.

5.3 Torque transients

The second sequence of experimental tests consists of torque trajectories composed of increasing and decreasing torque requests. These experiments are conducted at constant engine speed of 1000 rpm (Figure 7). The reference control strategy (named "ref") and the proposed control strategy (named "strat") are compared.

The low-level control variables (the intake BGR and the VVA actuator) are given in Figure 7(c) and Figure 7(d).

The intake manifold BGR is controlled by its low-level controller. It behaves similarly with the two different control strategies ("ref" and "strat",respectively). Yet, the VVA actuator trajectories are strongly different in the two cases. Indeed, in the case of the reference controller, the VVA trajectory Φ_{vva}^{sp} is only based on a static look-up table depending on the engine operating point. By contrast, in the proposed strategy, the VVA trajectory $\overline{\Phi_{vva}}$ is continuously updated during transients to satisfy the cylinder BGR objective. This can be seen in Figure 7(e) where the cylinder BGR tracks well its set point (which is not the case for the reference controller). Simultaneously, the cylinder temperature drifts away from its set point due to the change in the EGR/IEGR trade-off (see Figure 7(f)). Finally, Figure 7(b) gives results on NO_x emissions. One can see that the whole system tends to move closer to the steady-state conditions with the proposed strategy. This permits to prevent the undesired NO_x emissions peaks during torque tips-in (especially during increasing intake manifold BGR demands).

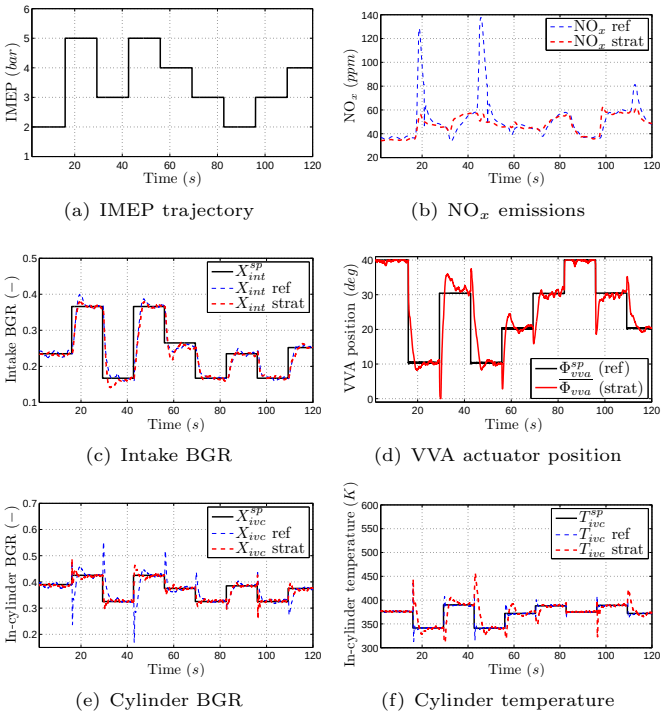

(a) IMEP trajectory (b) NO_x emissions

(c) Intake BGR (d) VVA actuator position

(e) Cylinder BGR (f) Cylinder temperature

Fig. 7. Test-bench results for a four-cylinder Diesel engine for step torque demand at constant speed of 1000 rpm with and without the proposed control strategy. The controller succeeds in tracking the cylinder BGR set point. Consequently, the NO_x emissions peaks are reduced.

6. CONCLUSIONS

A control strategy specifically designed to handle transients of turbocharged Diesel engines equipped with VVA actuator and LP EGR loop has been presented.

To reduce pollutant emissions, we control the BGR contained in the combustion chamber at ivc. A model of cylinder BGR and temperature has been presented. It uses a breathing model along with a dilution and a combustion

models. This model is shown to have interesting invertibility properties from which a control strategy has been developed. The strategy permits to accelerate the cylinder BGR response by coordinating the two variables acting on the breathing process, i.e. the intake manifold BGR and the position of the VVA actuator.

Experimental results obtained on a test bench have stressed the relevance of the control strategy. A significant reduction of the NO_x emissions during transients has been obtained.

ACKNOWLEDGEMENTS

The authors would like to gratefully thank Gilles Corde, Philippe Moulin and Jérémy Malaizé for their scientific support and David Bizien for his contribution to the experiments.

REFERENCES

Bression, G., Pacaud, P., Soleri, D., Cessou, J., Azoulay, D., Lawrence, N., Doradoux, L., and Guerrassi, N. (2008). Comparative study in LTC combustion between a short HP EGR loop without cooler and a variable lift and duration system. In *17th Aachen Colloquium*.

Chauvin, J., Corde, G., Petit, N., and Rouchon, P. (2008). Motion planning for experimental airpath control of a Diesel homogeneous charge-compression ignition engine. *Control Engineering Practice*, 16, 1081–1091.

Chauvin, J. and Petit, N. (2007). Experimental control of variable cam timing actuators. In *Proc. of International Federation of Automatic Control (IFAC) Symposium on Advances in Automotive Control*, volume 5.

Genç, A., Glover, K., and Ford, R. (2001). Nonlinear control of hydraulic actuators in variable cam timing engines. In *International IFAC Workshop on Modeling, Emissions and Control in Automotive Engines*.

Heywood, J. (1988). *Internal Combustion Engine Fundamentals*. McGraw-Hill, Inc.

Jankovic, M. and Kolmanovsky, I. (1998). Robust nonlinear controller for turbocharged Diesel engines. In *Proc. of the American Control Conference*, volume 3, 1389–1394.

Lancefield, T., Lawrence, N., Ahmed, A., and Ben Hadj Hamouda, H. (2006). VLD a flexible, modular cam operated VVA system giving variable valve lift and duration and controlled secondary valve openings. In *SIA-IFP*.

Leroy, T., Bitauld, M., Chauvin, J., and Petit, N. (2009). In-cylinder burned gas rate estimation and control on VVA Diesel engines. In *Proc. of the Society of Automotive Engineering World Congress*, 2009-01-0366.

Rausen, D., Stefanopoulou, A., Kang, J., Eng, J., and Kuo, T. (2005). A mean-value model for control of homogeneous charge compression ignition (HCCI) engines. *Journal of Dynamic Systems, Measurement, and Control*, 127(3), 355–367.

Throop, M. and Cook, J. (1985). The effect of EGR system response time on NO_x feedgas emissions during engine transients. *SAE Transactions*, 94(1), 1844–1853.

Toda, T., Nohira, H., and Kobashi, K. (1976). Evaluation of burned gas ratio (BGR) as a predominant factor to NO_x. In *Proc. of the Society of Automotive Engineering World Congress*, 760765.

Van Nieuwstadt, M., Kolmanovsky, I., Moraal, P., Stefanopoulou, A., and Jankovic, M. (2000). Experimental comparison of EGR-VGT control schemes for a high speed Diesel engine. *Control System Magazine*, 20, 63–79.

Wang, J. (2008). Air fraction estimation for multiple combustion mode Diesel engines with dual-loop EGR systems. *Control Engineering Practice*, 16(12), 1479–1486.

Appendix A. EXHAUST MODELING

A.1 Exhaust BGR modeling

Assuming complete and lean combustion, the exhaust BGR only depends on the composition inside the cylinder before the combustion (at *ivc*) and on the quantity of injected fuel, it comes

$$X_{exh}(k+1) = X_{ivc}(k) + \frac{(\mathrm{AFR}_s + 1) \cdot m_f(k)}{m_{ivc}(k)} \quad \text{(A.1)}$$

where X_{ivc} and m_{ivc} are the cylinder BGR and mass at *ivc*, respectively. m_f is the injected fuel mass, and AFR_s is the stoichiometric air/fuel ratio. The cylinder mass writes (see Leroy et al. (2009)) $m_{ivc} = \alpha_1(P_{int}V_{ivc})/(RT_{ivc})$, then substituting into (A.1), one finally obtains

$$X_{exh}(k+1) = X_{ivc}(k) + \frac{(\mathrm{AFR}_s + 1) \cdot m_f(k) R}{\alpha_1 P_{int}(k) V_{ivc}} T_{ivc}(k) \quad \text{(A.2)}$$

A.2 Exhaust temperature modeling

We assume an adiabatic compression, an instantaneous heat release and a polytropic expansion. After exhaust valve closing, the exhaust temperature of the gas leaving the cylinder during the exhaust blowdown is given by the adiabatic expansion of the gas from the combustion chamber to the exhaust manifold. Noting T_{bd} the exhaust temperature during the exhaust blowdown, and using the cylinder mass expression given above, one obtains (see Rausen et al. (2005))

$$T_{bd} = T_{ivc} \left(\frac{P_{exh}}{\alpha_1 P_{int}} \right)^{\frac{\gamma-1}{\gamma}} \left(1 + \mu_1 \frac{R Q_{LHV} m_f}{\alpha_1 c_v V_{ivc} P_{int}} \right)^{\frac{1}{\gamma}}$$

where $\mu_1 = \left(\frac{V_{comb}}{V_{ivc}}\right)^{\gamma-1}$ with V_{comb} the cylinder volume when combustion appears. To simplify the model, V_{comb} can be taken as constant. Finally, taking into account the heat losses in the exhaust runner (as is done in Rausen et al. (2005), e.g.), the dynamics of the temperature in the exhaust manifold can be written as

$$T_{exh}(k+1) = \mu_2 T_{ivc}(k) \left(\frac{P_{exh}(k)}{\alpha_1 P_{int}(k)} \right)^{\frac{\gamma-1}{\gamma}} \cdot \left(1 + \mu_1 \frac{R Q_{LHV} m_f(k)}{\alpha_1 c_v V_{ivc} P_{int}(k)} \right)^{\frac{1}{\gamma}} \quad \text{(A.3)}$$

where $\mu_2 < 1$ is a positive constant.